In Vitro Quantification of Guidewire Flow-Obstruction Effect in Model Coronary Stenoses for Interventional Diagnostic Procedure

Koustubh D. Ashtekar
Department of Mechanical Engineering,
University of Cincinnati,
Cincinnati, OH 45221

Lloyd H. Back
Jet Propulsion Laboratory,
California Institute of Technology,
Pasadena, CA 91125

Saeb F. Khoury
Department of Internal Medicine-Cardiology,
University of Cincinnati,
Cincinnati, OH 45221

Rupak K. Banerjee[1]
Associate Professor
Departments of Mechanical Engineering
and Biomedical Engineering,
University of Cincinnati,
Cincinnati, OH 45221
e-mail: rupak.banerjee@uc.edu

The objective is to quantify the guidewire (diameter of 0.35 mm) flow-obstruction effect in the in vitro model coronary stenoses in relation to trans-stenotic pressure drop, Δp, fractional flow reserve (gFFR; "g" represents FFR measurement with guidewire insertion) and coronary flow reserve (gCFR) for steady and pulsatile physiological flows. The sensor tipped pressure or flow measuring guidewire insertion through stenotic lumen increases the trans-stenotic pressure drop or reduces the pharmacologically induced hyperemic flow in the coronary arteries with plaques. These hemodynamic changes may cause error in true FFR and CFR measurements, especially for intermediate coronary stenosis. To quantify guidewire flow-obstruction effect, simultaneous measurements of trans-stenotic pressures and flow were performed by two methods: (a) guidewire based measurements (gCFR and gFFR by inserting sensor tipped guidewire) and (b) true physiological measurements (CFR by in-line Doppler flow cuff and FFR by the radially drilled pressure ports in three epicardial coronary stenotic test sections, postangioplasty, intermediate, and preangioplasty). The diagnostic parameters measured before guidewire insertion (CFR and FFR) and during guidewire insertion (gCFR and gFFR) were validated numerically and correlated with the new diagnostic parameter "lesion flow coefficient (LFC)." There was significant flow reduction with increased trans-stenotic pressure drop due to guidewire insertion. The FFR-gFFR and CFR-gCFR correlations were FFR$=0.92\times$gFFR$+0.097$ ($R^2=0.99$) and CFR$=0.91\times$gCFR$+0.44$ ($R^2=0.99$), respectively, where gCFR is reported from clinical pressure-flow data. Similar highly regressed ($R^2>0.9$) correlations were obtained for LFC and gLFC with flow ratios and pressure ratios. There was significant difference between steady and pulsatile pressure drops for the same mean flow with and without guidewire insertion. The trans-stenotic hemodynamics was altered due to guidewire insertion. The true FFR and CFR were underestimated because of guidewire insertion. Hence, the FFR-gFFR and CFR-gCFR correlations can be used to find out true FFR and CFR from clinically measured values (i.e., gFFR and gCFR). In addition, the gLFC-gCFR and gLFC-gFFR were correlated significantly for post- and preangioplasty conditions. [DOI: 10.1115/1.2776336]

Keywords: hemodynamics, guidewire diagnostic, transstenotic pressure drop, lesion flow coefficient (LFC), intermediate stenosis

Introduction

To assess the hemodynamic severity of angiographically moderate coronary stenosis, hemodynamic parameters such as fractional flow reserve (gFFR) [1] and coronary flow reserve (gCFR) [2] ("g", clinical measurement with guidewire insertion) are measured widely in contemporary clinical methods. The small diameter pressure and/or flow sensor tipped guidewires [3] (diameter of 0.014 in., i.e., 0.35 mm) are advanced through the stenosis into the distal vessel to measure the distal hyperemic pressure, $\tilde{p}_{rh}$ ("~" is the mean or time averaged quantity for pulsatile flow) and gFFR is determined by the ratio $\tilde{p}_{rh}/\tilde{p}_a$, where $\tilde{p}_a$ is aortic pressure measured by guiding catheter [1,4,5]. A typical range of gFFR is

$0.36<$gFFR<1; gFFR$\rightarrow 1$ means $\tilde{p}_{rh}\rightarrow\tilde{p}_a$, which signifies less severe stenosis. In contrast, gFFR<0.75 means significant stenosis, which may cause ischemia. The trans-stenotic pressure drop is given as $\Delta\tilde{p}=\tilde{p}_a-\tilde{p}_{rh}$ [6–9]. Similarly, intracoronary Doppler flow velocity measurement is performed with Doppler flow sensor tipped guidewire [10] and gCFR is calculated by the ratio of pharmacologically induced hyperemic flow ($\tilde{Q}_h$) to basal coronary flow ($\tilde{Q}_b$). A typical range of gCFR is $1<$gCFR<4; gCFR$\rightarrow 1$ means that there is no hyperemic response to the vasodilator drugs, i.e., severe stenosis. In contrast, gCFR$\rightarrow 4$ means that there is four times increase in basal flow due to vasodilators, indicating insignificant stenosis.

Potential risks and resulting consequences to the patients because of uncertainties in the pressure drop and flow measurements due to the size of the catheters and guidewires were reported by clinicians. Many clinicians had reported elevated physiological pressure drop (in clinical procedure, this is often referred to as pressure gradient) due to guidewire insertion [6,7]. These pressure

drops were measured with large diameter angioplasty catheters (diameter of 1.4 mm) causing "tight fit" in the lumen of the stenosed artery, as explained analytically by Back et al. [11]. The initial use of miniaturized guidewire of diameter 0.45 mm in 15 patients before angioplasty [12] had demonstrated the increase in the pressure drop due to guidewire (32 mm Hg and 44 mm Hg for systole and diastole, respectively) and conventional balloon angioplasty catheter placement (77 mm Hg and 59 mm Hg for systole and diastole, respectively), confirming the uncertainty of pressure drop measurement due to the size of catheter or guidewire. Hence, we are interested in more accurate quantification of the guidewire flow-obstruction effect on $\Delta \tilde{p}$, FFR, and CFR in an in vitro experimental setup with the commonly used guidewire size of 0.35 mm.

Very few in vitro experimental studies reported the guidewire flow-obstruction effect. De Bruyne et al. [8] showed that the guidewire of diameter 0.38 mm affects the trans-stenotic hemodynamics with 20% overestimation of pressure drop in the severe stenosis with >90% area reduction. The increased flow resistance due to angioplasty catheter insertion was studied for a wide range of ratios of catheter diameter to coronary vessel diameter: 0.3–0.7 [13]. The flow resistance was increased by a factor of 3–33 for concentric configuration, indicating the importance of quantifying the catheter obstruction effect. A guidewire insertion changed the "averaged peak velocity (APV) versus time averaged mean velocity" relation in the throat region of stenosis, resulting in underestimation of true CFR [14].

All these in vitro studies had used Newtonian blood analog fluid and steady flow, which are physiologically inappropriate. Moreover, the guidewire flow-obstruction effect should be accurately quantified in intermediate stenosis zone in order to accurately diagnose the patients under "gray zone."[2] Hence, coronary stenosis hemodynamics is examined in detail to find out the effect of guidewire insertion on FFR and CFR in this in vitro experiment replicating clinical settings. This in vitro study reports more accurate results with realistic pulsatile flow using non-Newtonian blood analog fluid and compares the results with steady flow measurements. The newly developed diagnostic parameter, lesion flow coefficient (LFC), is also evaluated and compared with gFFR and gCFR [16]. The LFC considers the guidewire size in relation to the minimum lumen diameter along with pressure drop and flow. Hence, gLFC is calculated and again compared with $\tilde{p}_r/\tilde{p}_a$ and $\tilde{Q}/\tilde{Q}_b$ when the guidewire is inserted. At hyperemic flow, $\tilde{p}_r/\tilde{p}_a$ =gFFR and $\tilde{Q}/\tilde{Q}_b$=gCFR.

Materials and Methods

In order to evaluate $\Delta \tilde{p}$, CFR, gCFR, FFR, gFFR, LFC, and gLFC before and during the guidewire insertion, a 1:1 bench top experimental setup and stenosis test sections are developed. The experimental setup and numerical methods are discussed as below.

In Vitro Experiments. *Test section*. The coronary stenosis test sections are manufactured with optical grade Lexan material (σ_u =65 MPa, Rockwell hardness=R118, water absorption at saturation=0.35%) for three different geometries: postangioplasty, intermediate, and preangioplasty, i.e., 64.8%, 80%, and 89% area stenosis, respectively. Figure 1(a) shows the photograph of postangioplasty stenosis test section, illustrating three distinct regions: converging, throat, and diverging sections. The dimensions are based on clinical measurements and are shown in Table 1 [6,11]. Figure 1(b) shows the MicroCT (Imtek Inc., TN) images of intermediate and preangioplasty stenosis test sections, edited in IMAGEJ software (National Institutes of Health, MD) to find out exact geometric dimensions. To measure true trans-stenotic pressure

without guidewire insertion, 0.3 mm diameter pressure ports are drilled radially along the stenotic test sections so that the pressure in the axial direction of the stenosis can be measured, as shown in Fig. 1(a). The MicroCT images in Fig. 1(b) are taken only for "stenotic portion" of the test section and hence they do not show all pressure ports.

In vitro flow loop. The flow circuit (Fig. 2) is designed to simulate the physiological flow profile proximal to the stenosis test section [17], as shown in Fig. 3. Glycerin-water solution prepared with 65% water+35% glycerin+0.02% xanthan gum by weight [18] is used as blood analog fluid (BAF), showing typical shear thinning non-Newtonian viscosity [19]. The typical range of magnitude of shear rates for coronary artery of 3 mm diameter with physiological blood flow velocity is 0–1000 s^{-1}. For this range of shear rate, the dynamic viscosity of real blood, μ, varies from 56 cP to 4 cP [19]. The viscosity data are regressed to the non-Newtonian viscous Carreau model, where zero shear rate viscosity μ_0=55.72 cP, infinite shear rate viscosity μ_∞=3.39 cP, time constant λ=9.62 s, and power index n=0.2. The BAF is stored in the overhead fluid storage tank, which is about 1 m above the level of test section. This tank generates enough driving pressure of 80 mm Hg in the flow circuit. The basic pulsatile flow, similar to the aortic flow profile, is generated by blood pump (Harvard apparatus, MA). The flow is then bifurcated into two tubes with two compliance chambers (C1 and C2) and resistances (R1 and R2). The desired flow profile is obtained by (1) maintaining a certain fluid column height in C1 and C2, (2) modifying resistances R1 and R2, and (3) the pump parameters, such as time period, systole to diastole flow ratio, and stroke length. Thus, coronary flow pulse with diastolic predominance is generated in the in vitro setup with a time period of 0.8 s (Fig. 3).

To observe the guidewire flow-obstruction effect and to quantify the overestimation of pressure drop, the pulsatile flow rate and trans-stenotic pressures are measured simultaneously for two conditions: with and without insertion of guidewires. These conditions are discussed below.

(1) In true physiological pressure-flow measurements, pressure measurements are conducted using pressure ports drilled radially to the axial flow direction in the stenosis test section. The pressure ports are connected to a digital pressure scanner (Scanivalve Corp., WA), which acquire pressure data at every 12 ms time interval. These measurements are taken without insertion of guidewire. Hence, the pressure drop measured with this method is designated as a true physiological $\Delta \tilde{p}$.

(2) In guidewire based pressure-flow measurements, the pressure sensor tipped guidewire (diameter of 0.35 mm) is advanced distal to the stenosis using a rotating hemostatic valve to measure $\tilde{p}_r$. The sensor tip is placed over the distance Δz distal to the stenosis, where complete pressure recovery is observed. The proximal pressure $\tilde{p}_a$ is recorded by a digital pressure scanner with proximal pressure port. The $\tilde{p}_r$ is recorded using the Combomap system (Volcano Therapeutics, CA). This method acquires the physiological pressure measurements in clinical settings. Hence, the pressure drop measured with this method is designated as a guidewire based $\Delta \tilde{p}$.

The flow is measured by in-line Doppler flow sensor (Transonic Inc., NY) at the intervals of 1 ms. The true trans-stenotic pressure and flow are measured simultaneously. The flow and pressure data are recorded using the data acquisition system (National Instruments, TX). Later, the pressure data are analyzed to obtain trans-stenotic pressure drop and time period of pulse, T, by visual basic program.

Experimental protocol. After calibration of all measuring instruments, the steady flow experiment is performed. The gravity induced steady flow is generated by overhead tank. The steady

---

[2]Gray zone is defined as the coronary stenosis for which FFR measurement is between 0.75 and 0.8 [15].
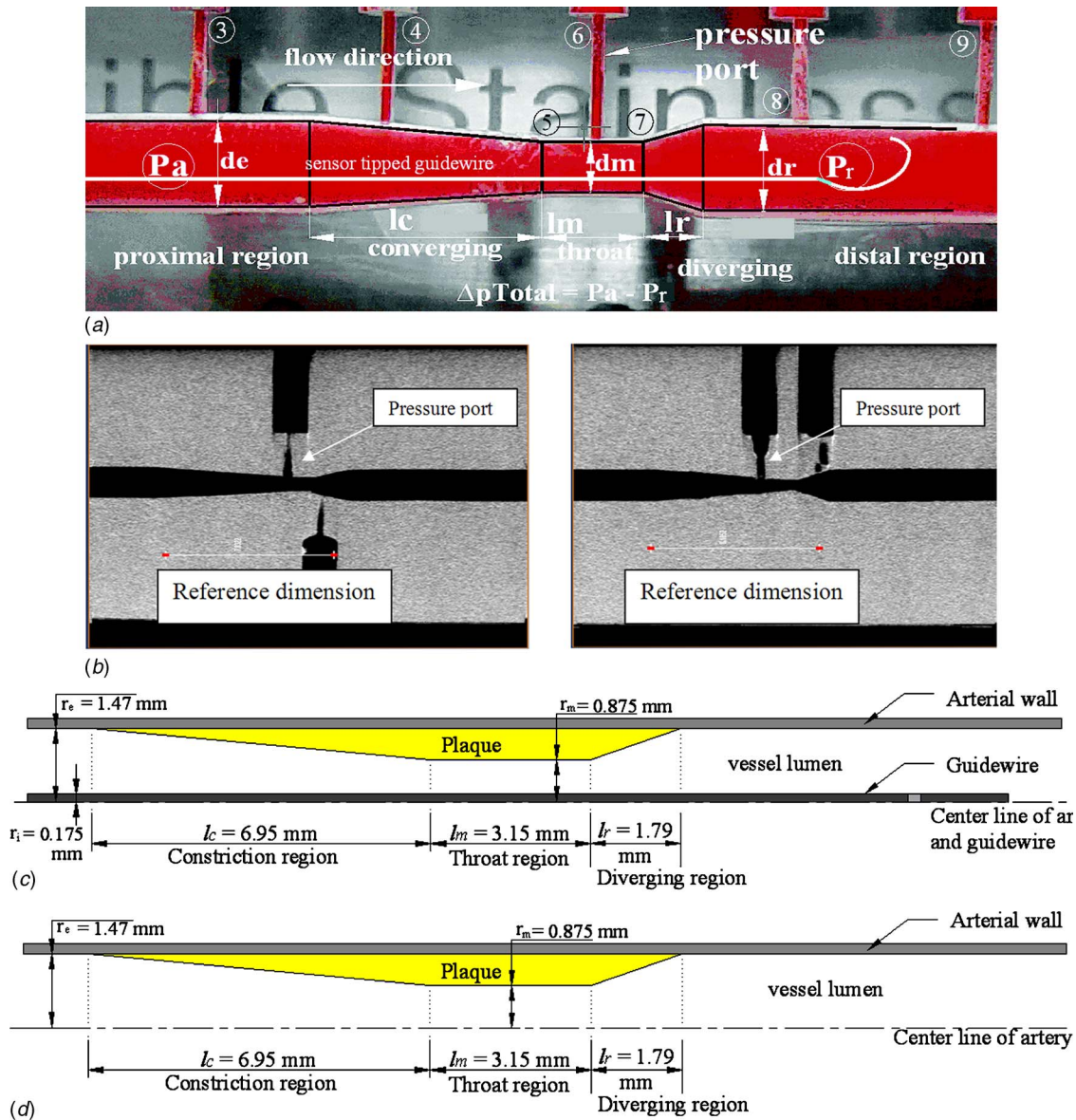
Fig. 1 (*a*) Photograph of postangioplasty stenosis test section. A total of 16 pressure ports (diameter of 0.3 mm) is drilled radially along the axial direction of stenosis test section, spaced approximately 5 mm apart. Port No. 3 is located 3.4 mm proximal to the converging section. Port Nos. 5 and 7 are drilled on the opposite side of the shown face and are located at the start and at the end of throat section, respectively. (*b*) MicroCT images of intermediate and preangioplasty stenotic test sections. The picture is taken only for 2 cm in proximity to the stenosis test section. Port Nos. 4 and 5 are shown in this figure. A total of 16 and 14 pressure ports is drilled radially for intermediate and preangioplasty stenotic test sections, respectively. (*c*) Schematic diagram of stenosis test sections with inserted guidewire for postangioplasty case. (*d*) Schematic diagram of stenosis test sections without inserted guidewire for postangioplasty case.

flow, Q is varied from a basal flow rate of 50 ml/min ($\sim \text{Re}_e = 111$) to a hyperemic flow of 125 ml/min ($\sim \text{Re}_e = 278$) for preangioplasty and 180 ml/min ($\sim \text{Re}_e = 400$) for postangioplasty by varying resistances R1 and R2 and keeping capacitances C1 and C2 zero, thus increasing the flow in four steps. The corresponding steady state pressure drops are measured with and without guidewire insertion. The reduced flow rate and elevated pressure drops are measured by both guidewire connected to the Combomap system and digital pressure scanner. To gauge the degree of guidewire obstruction during wire insertion, only external pressure scanner data are used throughout the experimental protocol. However, the guidewire based pressure readings are compared with digital pressure scanner data for confirmation only.

Next, pulsatile flow experiment is performed for the same

stenosis test section. The pulsatile flow is obtained by varying C1 and C2 in addition to R1 and R2 as explained previously. The mean pulsatile flow rate is also varied in four steps from basal to hyperemic level. A similar procedure, adapted for the steady flow experiment, is used for guidewire based and true trans-stenotic pulsatile pressure and flow measurements. A total of three experiments is performed ($n = 3$). Similarly, all stenosis test sections are tested and the guidewire flow-obstruction effect with pressure drop overestimation is observed. Further, the data sets are analyzed for CFR, gCFR, FFR, gFFR, LFC, and gLFC.

Numerical Method. To validate the experimental data, the guidewire flow-obstruction effect is numerically calculated. Two numerical models are created: (1) true physiological flow condi-

Table 1 Dimensions for three test sections: preangioplasty, intermediate, and postangioplasty. All dimensions are measured with IMAGEJ software. The dimensions and shape of the pre- and postangioplasty stenoses were obtained from quantitative biplanar angiography [6,11]. The dimension of intermediate stenosis is taken by considering the axial redistribution of plaque during the balloon angioplasty. Postintervention stenoses are typically 5–20% and the minimal lesion diameter of the vessel depends on the extent of angioplasty procedure. Based on the clinical evidences found by Wilson et al. [6], postintervention minimal cross-sectional area was 2.5 mm², i.e., 1.78 mm diameter. The average diameter of vessel proximal to the stenosis was 3 mm, which makes the % area stenosis as 65%.

Sr. No.	Dimensions (mm)	89% area blockage (preangioplasty)	80% area blockage (intermediate)	64.8% area blockage (postangioplasty)
1	d_e	2.96	2.95	2.95
2	l_c	6.28	6.35	6.96
3	d_m	0.98	1.32	1.75
4	l_m	0.39	0.95	3.15
5	l_r	1.59	1.62	1.79
6	d_r	3.00	2.98	2.95

tion and (2) guidewire inserted condition, where the guidewire is considered as concentric with lumen walls. The numerical models are constructed based on the dimensions measured by MicroCT (Table 1). The stenotic arterial walls are assumed as rigid from basal to hyperemic flow conditions. The numerical models with dimensional details are given in Figs. 1(c) and 1(d). It is assumed that the stenosis model geometries are axisymmetric. The computational methodology is based on guidelines reported by Banerjee et al. [20].

The non-Newtonian fluid flow through the stenosis geometry is modeled as unsteady hemodynamics with shear layer instabilities for a pulse time period of ~0.8 s [20–22]. The corresponding governing Navier–Stokes equations are solved by finite element method, utilizing Galerkin formulation. The mesh and transient time increment are used with proper care as explained by Banerjee et al. [20] for both steady and pulsatile flow problems. The boundary conditions for these models are as follows.

1. Without guidewire insertion (Fig. 1(d)). The axisymmetric
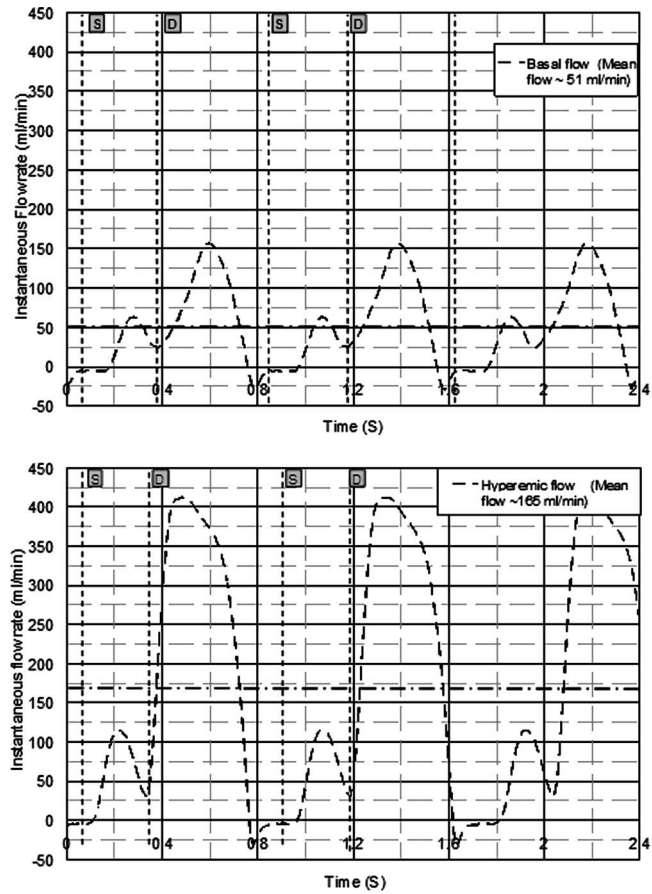
Fig. 3 Hyperemic and basal pulsatile flow versus time generated in the flow loop and applied to the test section. S, start of systole; D, start of diastole. The flow wave form obtained in the in vitro experiment is based on the flow wave form obtained by in vitro calibration (Cho et al. [17]).

condition ($v_r=0$) is applied at the centerline. No-slip ($v_r,v_z=0$) boundary condition along the arterial wall and stress free boundary condition at the flow outlet are applied. The flow is allowed to develop for a length of 25 mm proxi-
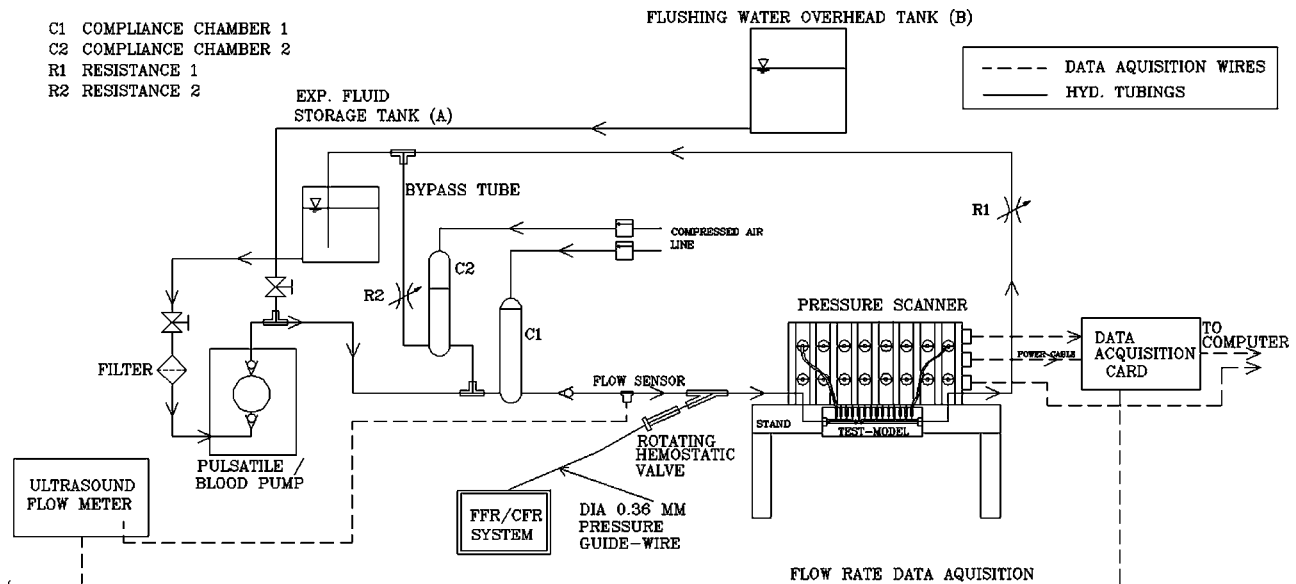
Fig. 2 Experimental setup showing the flow loop, data acquisition system, and stenotic test section

mal to the stenosis with non-Newtonian fluid viscosity. A transient Poiseuille flow inlet boundary condition at each time step is applied with a subroutine. A detailed description of numerical methodology is provided in our earlier publications [20].

2. With guidewire insertion (Fig. 1(c)). The annulus formed between the guidewire and lumen wall is modeled with no-slip boundary condition at the artery wall and guidewire surface along with stress free boundary condition at the flow outlet. The corresponding Poiseuille flow inlet boundary condition for flow through circular annulus is applied with a subroutine. The flow is allowed to develop for a length of 25 mm proximal to the stenosis with non-Newtonian fluid viscosity.

Results

The effects of guidewire insertion on coronary hemodynamics are studied and presented for steady and pulsatile flow conditions. The results are presented in terms of overestimated pressure drop, reduction in mean coronary hyperemic flow rate and reduction in hyperemic distal coronary pressure, $\tilde{p}_{rh}$, and resultant effect on physiological true FFR and CFR. These experimental data are validated with subsequent numerical calculations. The newly introduced diagnostic parameter, LFC, is experimentally evaluated for preangioplasty and postangioplasty stenosis test sections with and without 0.35 mm guidewire insertion.

Pressure Drop-Flow ($\Delta p - Q$) Characteristic. *Steady flow*. Figure 4(b) shows the $\Delta p - Q$ characteristic of steady flow experiments for all stenosis test sections with and without guidewire insertion. The quadratic curve fitted relation $\Delta p = AQ^2 + BQ$ for each % area stenosis is shown in Fig. 4(b) by solid lines for experimental data, along with the dashed lines for numerical results. The first quadratic term in the above equation represents the momentum-change pressure drop and the second linear term represents the viscous pressure drop [16,23]. There is an order of magnitude decrease in the momentum-change coefficient A and relatively small decrease in the viscous coefficient B when stenosis severity decreased from preangioplasty to postangioplasty. These variations indicate that the preangioplasty stenosis is momentum change (or flow separation) dominated and the postangioplasty stenosis is viscous (friction) dominated.

Pulsatile flow. Figure 4(c) shows the $\Delta \tilde{p} - \tilde{Q}$ ("~" indicates the time averaged quantities of pulsatile hemodynamic parameters) characteristic for pulsatile flow experiments. The analogous quadratic relation for pulsatile flow, $\Delta \tilde{p} = A\tilde{Q}^2 + B\tilde{Q}$, is obtained for each stenosis test section with the numerical validations using dashed lines. These plots provide comparison of momentum change associated energy loss and viscous loss for three % area stenosis before and after guidewire insertion. The pulsatile flow increases the momentum-change pressure losses for all stenosis conditions as compared with steady flow condition. However, guidewire insertion increases the momentum-change as well as viscous pressure losses for pulsatile flow conditions. A typical recorded trans-stenotic axial pressure $p(t)$ measured by inserting the pressure guidewire is shown in Fig. 4(a).

Determination of Hyperemic Flow. The physiological flow conditions such as arterial compliance and pharmacologically induced hyperemia cannot be achieved in an in vitro experimental setup. The maximum limiting hyperemic flow rate confirming clinically measured gCFR is obtained from CFR$-\tilde{p}_{rh}$ line [24]. The distal recovered pressure $\tilde{p}_r$ is calculated for each flow and stenosis test section by the relation $\tilde{p}_r = \tilde{p}_a - \Delta \tilde{p}$. Substituting for $\Delta \tilde{p}$, we get $\tilde{p}_r = \tilde{p}_a - A\tilde{Q}^2 - B\tilde{Q}$, i.e., relation between $\tilde{p}_r$ and $\tilde{Q}$. Proximal aortic pressures $\tilde{p}_a$ are assumed as 84 mm Hg for postangioplasty, 86 mm Hg for intermediate stenosis, and 89 mm Hg for preangioplasty (Table 2). Figure 5 shows the nondimensional-

ized parameter $\tilde{Q}/\tilde{Q}_b$ (this ratio is CFR at hyperemic flow, $\tilde{Q}_h$) versus $\tilde{p}_r$, where $\tilde{Q}_b$ is the mean basal flow rate of 50 ml/min for all stenoses during guidewire based and true physiological measurements [25]. The physiological limiting conditions are imposed on the plots in Fig. 5 by CFR$-\tilde{p}_{rh}$ relation, which is based on the hemodynamic end points provided in Table 2 [6,26]. The relation CFR$=0.065 \times \tilde{p}_{rh} - 1.296$ was used to calculate hyperemic flows for all stenotic conditions.

By plotting CFR$-\tilde{p}_{rh}$ line from Table 2, the zero flow pressure, $\tilde{p}_{zf} \approx 20$ mm Hg, was obtained. The intersections of $\tilde{Q}/\tilde{Q}_b$ versus $\tilde{p}_{rh}$ curve and CFR$-\tilde{p}_{rh}$ line give physiological limiting conditions in terms of CFR or gCFR, i.e., guidewire measured flow rate, $\tilde{Q}_h = CFR\times \tilde{Q}_b$. The hyperemic flows calculated by this method for this experimental setup are summarized in Table 3 for pulsatile and steady flow conditions.

Guidewire Insertion Effect on Pressure Drop and Flow Measurements. Guidewire insertion overestimates the true physiological $\Delta \tilde{p}$, which is inversely dependent on the guidewire size relative to the minimal vessel lumen size, i.e., d_g/d_m. The true % area stenoses are increased from 64.8%, 79.9%, and 89% to 65.7%, 81.2%, and 90.3% for postangioplasty, intermediate, and preangioplasty stenoses, respectively, due to guidewire insertion. Though the increment in % area stenosis seems to be less, the guidewire flow obstruction and overestimation of pressure drop are more significant for preangioplasty than postangioplasty condition. Thus, the contribution of guidewire flow obstruction increases the as the % area or diameter stenosis increases. For pulsatile flow conditions, increases in hyperemic pressure drops (=guidewire based $\Delta \tilde{p}_h$−ture physiological $\Delta \tilde{p}_h$) are 1.6 mm Hg, 3.6 mm Hg, and 4.6 mm Hg for postangioplasty, intermediate, and preangioplasty stenoses, respectively. Similarly, for steady flow conditions, increases in hyperemic pressure drops (=guidewire based Δp_h−ture physiological Δp_h) are 2.3 mm Hg, 4.1 mm Hg, and 5.4 mm Hg. For pulsatile flow conditions, reductions in hyperemic flows (=true physiological $\tilde{Q}_h$−guidewire based $\tilde{Q}_h$) are 5 ml/min, 12 ml/min, and 15 ml/min for postangioplasty, intermediate, and preangioplasty conditions, respectively. For steady flow, hyperemic flow reductions (=true physiological Q_h−guidewire based Q_h) are 7.5 ml/min, 13.5 ml/min, and 17.5 ml/min. The steady flow values of overestimated pressure drop and reduced flow are greater than those for pulsatile flow. As seen in the numerical analysis for pulsatile flow condition, the pressure is recovered significantly in the distal portion of the stenosis due to shear layer instabilities caused by the formation and breakup of organized vortical cells with time near the wall region in the diverging sections [20–22,25]. For steady flow condition, these vortices are formed and are sustained for longer length reducing the pressure recovery as compared with pulsatile flow case.

Guidewire insertion enhances the viscous losses because of the added surface area of the guidewire in the vessel lumen and also enhances the momentum-change pressure losses because of the reduced flow area. From the $\Delta \tilde{p} - \tilde{Q}$ relationship, the momentum-change pressure losses are scaled by $\tilde{Q}^2$ term and viscous pressure losses are scaled by $\tilde{Q}$ only. Also, from the observations of numerical steady and pulsatile cases, viscous losses are smaller than the momentum-change losses. Hence, in order to study the guidewire insertion effect on the hemodynamics, the dominant momentum-change losses are analyzed by evaluating changes in momentum-change coefficient A. When guidewire is inserted, A increased by 28% =$(0.000187−0.000146)/0.000146\times100$; for coefficients, please refer to Figs. 4(b) and 4(c), under steady flow and 17% under pulsatile flow condition for postangioplasty stenosis. Similarly, for preangioplasty condition, A increased by 60% under steady flow condition and 56% under pulsatile flow condi-
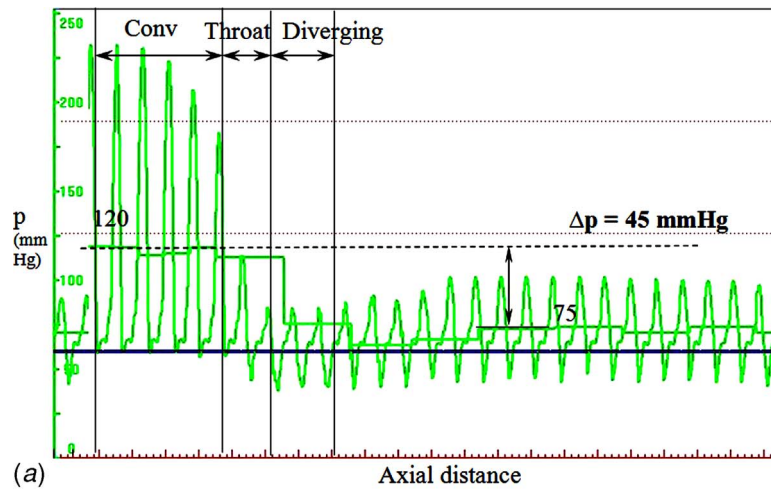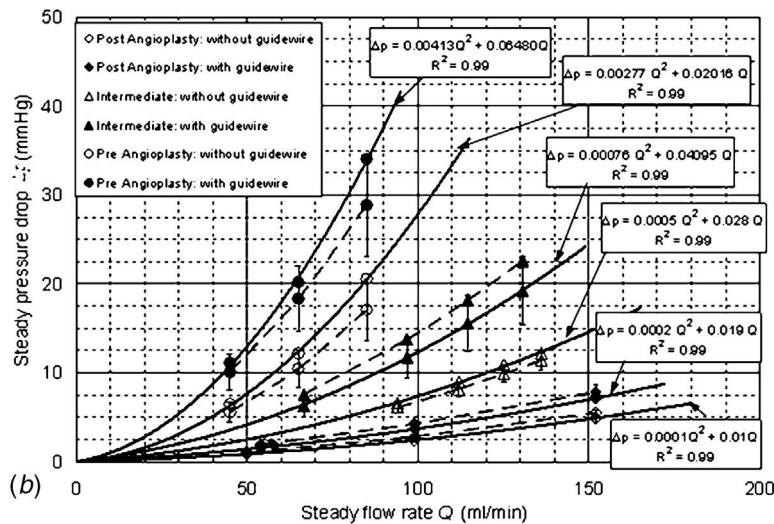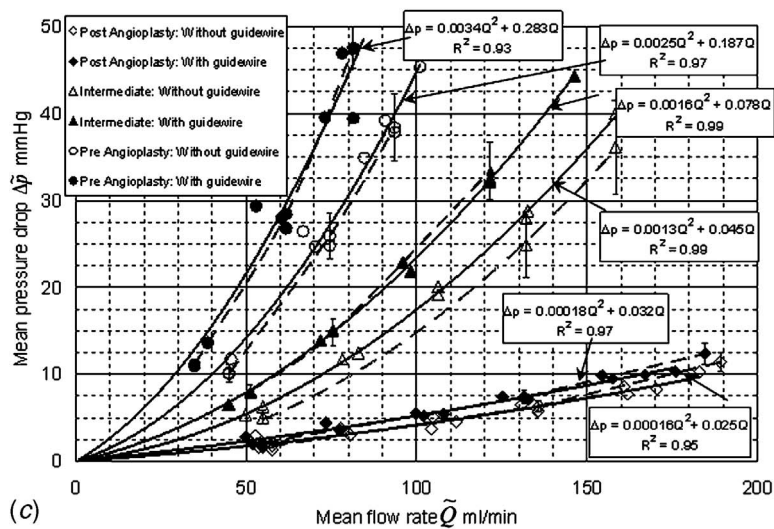
Fig. 4 (*a*) Pressure pulse at various times along the axial direction measured by Volcano system in converging, throat, and diverging sections. (*b*) Pressure drop versus flow characteristic for steady state experiment. (*c*) Time averaged pressure drop versus flow characteristic for pulsatile flow experiment. Legends: diamonds: postangioplasty; triangles: intermediate stenosis; and circles: preangioplasty. Filled data points: with guidewire insertion; unfilled data points: without guidewire insertion. The solid lines: second order polynomial curve fit for experimental data; the dashed lines: second order polynomial curve fit for numerical data. The *Y* axis scales are the same for comparison of steady and pulsatile flow condition pressure drops.

Table 2 Hemodynamic end points obtained from Refs. [6,26]. The in vitro data set is based on Wilson et al. [6] in vivo data, which was obtained from 32 patient group undergoing percutaneous transluminal coronary angioplasty (PTCA) with single-vessel, single-lesion coronary artery disease with stable or unstable angina pectoris.

Lesion	gCFR	$\tilde{p}_a$ (mm Hg)	$\Delta\tilde{p}_h$ (mm Hg)	$\tilde{p}_{rh}$ (mm Hg)	gFFR
Preangioplasty	2.3±0.1	89±3	34	55	0.62
Intermediate	3.3	86	14.3	70.4	0.82
Postangioplasty	3.6±0.3	84±3	7.4	75.2	0.89

tion. The lower % increase in A for pulsatile flow as compared with steady flow indicates that the larger pressure recovery distal to the stenosis occurs for pre- to postangioplasty cases. Also, the steady flow increases viscous pressure losses more predominantly than pulsatile flow. Hence, the overall viscous pressure drop is increased in the steady flow condition when the guidewire is inserted. In contrast, pulsatile flow increases momentum-change-related pressure losses. Hence, the overall momentum-change pressure drop is increased in the pulsatile flow condition when the guidewire is inserted. This increased momentum change elevates the organized vortical cell formation in the pulsatile flow condition, which recovers the pressure drop significantly as compared to the steady flow [20–22,25]. Thus, guidewire insertion changes trans-stenotic hemodynamics in different ways for steady and pulsatile flows.

The average difference between experimental and numerical pressure drop values is 4.3% whereas its range is 0.3–20%. The concentric configuration of guidewire placement, which is as-

sumed in numerical calculations, results in higher pressure drop (worst case scenario) than eccentric placement of guidewire across the stenosis, as in the case of experimental measurement, for the same mean flow rate (except for preangioplasty with steady flow). This explains that the concentric guidewire configuration alters the trans-stenotic hemodynamics differently as compared to eccentric configuration. The effect of eccentricity reduces as the % area stenosis severity increases [13]. Hence, the eccentricity effect can be considered important for postangioplasty stenosis only and its effect on intermediate and preangioplasty stenosis can be neglected. The other possible reasons for these differences are discussed in the Appendix.

Without guidewire, the pressure drop for pulsatile flow condition is larger than the pressure drop for steady flow in the case of intermediate and preangioplasty stenoses. For intermediate stenosis, a hyperemic flow of 128 ml/min is associated with pressure drops of 27 mm Hg for pulsatile and 12 mm Hg for steady flow
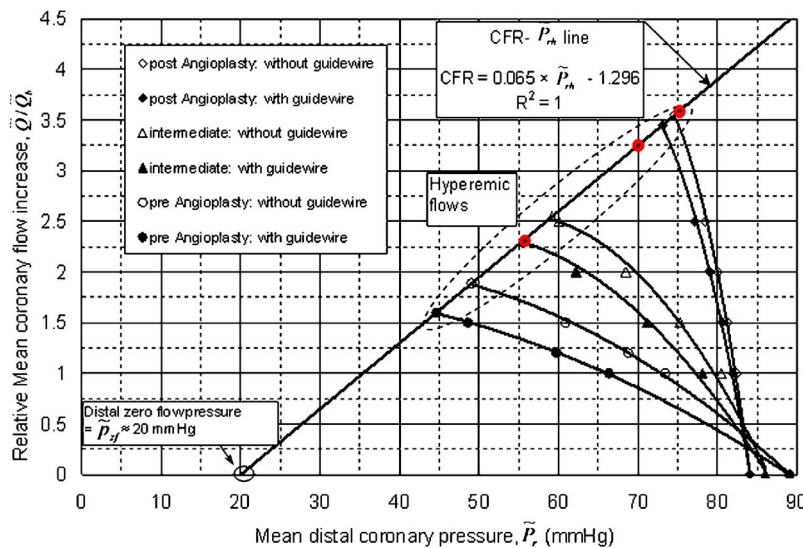
Fig. 5 CFR-p_{rh} line for mean pressure and flow data for pulsatile flow experiment. Hemodynamic hyperemic end points, as shown in Table 2, are represented by red donuts in the figure. The line connecting these three end points is used to limit the experimental data to calculate the hyperemic flows.

Table 3 Summary of basal and hyperemic flows for all stenoses. For all stenosis conditions, with and without guidewire inserted condition, basal flow is assumed as 50 ml/min, for both steady and pulsatile flow scenario [25].

|	Guidewire based hyperemic flow (with guidewire insertion)						True hyperemic flow (without guidewire insertion)					
	Steady flow			Pulsatile flow			Steady flow			Pulsatile flow		
	ml/min	Re_e	Re_m	ml/min	Re_e	Re_m	ml/min	Re_e	Re_m	ml/min	Re_e	Re_m
Preangioplasty	93	185	460	80	159	395	112	249	751	95	211	637
Intermediate	142	283	559	116	231	456	161	359	802	127	283	632
Postangioplasty	178	354	557	172	343	538	186	414	699	178	397	668
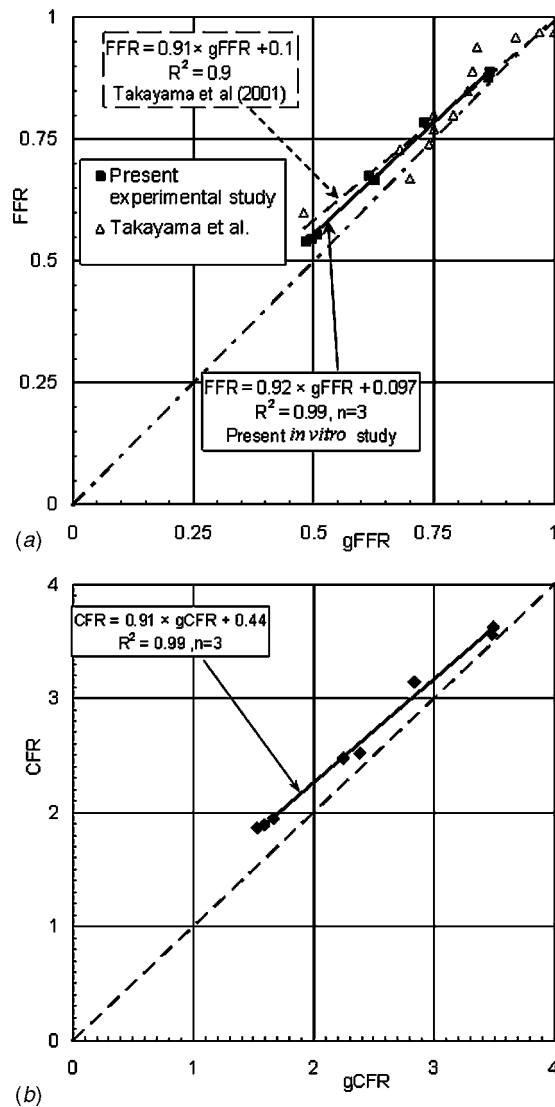
Fig. 6 (*a*) FFR-gFFR relation for pulsatile flow and (*b*) CFR-gCFR relation for pulsatile flow

conditions showing a 15 mm Hg difference. Similarly, for preangioplasty condition, a hyperemic flow of 95 ml/min is associated with pressure drops of 40 mm Hg for pulsatile and 27 mm Hg for steady flow conditions showing a 13 mm Hg difference. Unlike intermediate and preangioplasty characteristics, postangioplasty shows very negligible change in pressure drops, i.e., 9.3 mm Hg for pulsatile to 6.3 mm Hg for hyperemic flow of 178 ml/min. The pulsatile flow is considered to be a larger momentum-change loss ($\propto \tilde{Q}^2$) enhancer than viscous loss ($\propto \tilde{Q}$). Hence, intermediate and preangioplasty stenoses, which have higher momentum changes distal to the stenoses, have greater pressure drop differences between steady and pulsatile flows [16]. The postangioplasty has more viscous loss effects and thus, the pulsatile flow does not affect steady state pressure drop values significantly.

FFR-gFFR and CFR-gCFR Correlations. The FFR and CFR are evaluated for both true physiological and guidewire based methods. The gFFR is calculated by guidewire insertion and digital pressure scanner readings, and physiological true FFR is calculated from the digital pressure scanner data. Figure 6(*a*) shows the FFR—gFFR characteristic for all stenoses under pulsatile flow conditions. A highly regressed linear correlation between FFR and gFFR is obtained: FFR=0.92×gFFR+0.097 (R^2=0.99, n=3).

Previously, gFFR was measured in a group of 15 patients with clinically stable, single intermediate lesions in a native coronary vessel of diameter >2.5 mm [27]. In that study, FFR was measured by two methods: (a) inserting 0.014 in. diameter guidewire through 6F guiding catheter and (b) analytically calculating from stenotic dimensions measured by 3D intravascular ultrasound (IVUS). There is a good match between previously reported in vivo data [27] and present in vitro data, especially for intermediate stenosis region, as shown in Fig. 6(*a*).

A similar plot for CFR and gCFR is shown in Fig. 6(*b*) for pulsatile flow conditions, with highly regressed correlation CFR =0.91×gCFR+0.44 (R^2=0.99, n=3). The difference between FFR and gFFR as well as CFR and gCFR increases as severity of coronary stenosis increases. This confirms the fact that overestimation of pressure drop due to guidewire insertion is inversely dependent on the ratio of guidewire size to minimal lumen size (d_g/d_m) [13]. Using the Q/Q_b versus p_r curves with the same limiting CFR$-p_{rh}$ line for steady flow experimental data, FFR-gFFR and CFR-gCFR correlations are obtained (figure not shown in the paper). These correlations are FFR=0.91×gFFR+0.11 (R^2=0.99) and CFR=0.89×gCFR+0.56 (R^2=0.99). In physiological flow range for intermediate stenoses, where guidewire diagnostic is more uncertain, FFR-gFFR and CFR-gCFR correlations for steady and pulsatile flow conditions coincide with each other with maximum of 1.5% difference.

Even though there is relatively large difference between hyperemic pressure drops for steady and pulsatile flow experiments, FFR-gFFR and CFR-gCFR characteristics are similar. Depending on the distal pressure recovery, less pulsatile (or steady) flow may give different pressure drop than those for higher pulsatile flow. The arterial wall layer thickness, distribution of plaque in the lumen, and its effect on histology of the arterial tissues will change the elasticity of the artery and consequently the flow pulse shape. Also, the distal pressure is generally recovered largely during the diastolic phase of coronary flow, which may change hemodynamic end points of coronary ischemia from patient to patient.

LFC-CFR and LFC-FFR. The new diagnostic parameter, LFC, has been recently introduced by our group [16] for assessing coronary lesion severity. Unlike gFFR and gCFR, gLFC assesses simultaneous measurements of flow, pressure drop, and % area of stenoses under guidewire inserted condition. The LFC is defined as LFC=$[(1-\kappa)\tilde{Q}]/[(A_m-A_g)(2\Delta\tilde{p}/\rho)^{0.5}]$. The area measurement is introduced in the equation of LFC as κ. For guidewire based method, $\kappa=(A_m-A_g)/(A_e-A_g)$ and without guidewire case, $\kappa=A_m/A_e$. The LFC provides wide measure of hemodynamics in the stenosed coronary artery and hence proposed to assess the hemodynamic severity of coronary arterial stenosis.

The LFC and gLFC are evaluated for postangioplasty and preangioplasty conditions. Figure 7(*a*) shows LFC-FFR comparison, with and without guidewire insertion, which are well regressed with linear fit. For postangioplasty, the relations are gLFC= $-1.47\times {}_g(\tilde{p}_r/\tilde{p}_a)+1.79$ and LFC=$-1.69\times(\tilde{p}_r/\tilde{p}_a)+2.03$, whereas for preangioplasty, the relations are gLFC=$-0.28\times {}_g(\tilde{p}_r/\tilde{p}_a)^g$ +0.69 and LFC=$-0.32\times(\tilde{p}_r/\tilde{p}_a)+0.76$. At hyperemic condition, the ratio $\tilde{p}_r/\tilde{p}_a$ is defined as FFR or gFFR. For postangioplasty, gFFR of 0.9 corresponds to gLFC of 0.46; for preangioplasty, gFFR of 0.5 corresponds to gLFC of 0.55. Thus, as stenosis severity increases the gLFC increases, unlike gFFR. In preangioplasty stenosis condition, $\Delta\tilde{p}$ increases more nonlinearly due to momentum-change effect than that in postangioplasty stenosis. Hence, the denominator in the equation for gLFC is lower for preangioplasty than for postangioplasty condition. This explains the increase in gLFC from postangioplasty to preangioplasty conditions.

However, LFC is directly proportional to the CFR, as shown in Fig. 7(*b*). For postangioplasty, the relations are gLFC=0.065
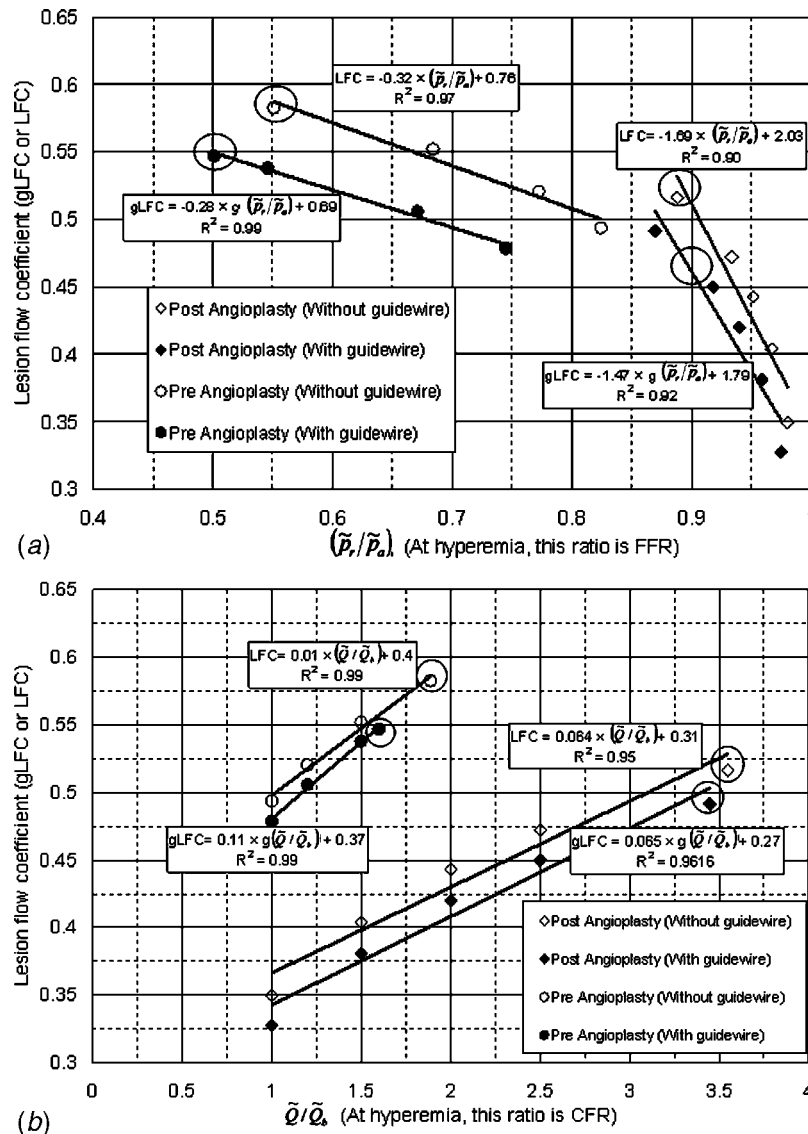
Fig. 7 (a) LFC-$(\tilde{p}_r/\tilde{p}_a)$ correlations. At hyperemia, circled points are FFR or gFFR. (b) LFC-$(\tilde{Q}/\tilde{Q}_b)$ correlations. At hyperemia, circled points are CFR or gCFR.

$\times_g(\tilde{Q}/\tilde{Q}_b)+0.27$ and LFC=$0.064\times(\tilde{Q}/\tilde{Q}_b)+0.31$. For preangioplasty condition, the correlations are gLFC=$0.11\times_g(\tilde{Q}/\tilde{Q}_b)+0.37$ and LFC=$0.01\times(\tilde{Q}/\tilde{Q}_b)+0.4$. These relations are highly regressed ($R^2>0.9$). At hyperemic condition, the ratio $\tilde{Q}/\tilde{Q}_b$ is defined as CFR or gCFR. For postangioplasty, gCFR of 3.0 corresponds to gLFC of 0.46; for preangioplasty, gCFR of 1.6 corresponds to gLFC of 0.55. Thus, it is possible to use gLFC (considering guidewire obstruction effect) to assess severity of coronary stenosis, instead of measuring two different parameters, gFFR and gCFR.

Discussion

Studies on the impact of guiding catheter and balloon angioplasty catheter for measuring intracoronary pressure concluded that the occurrence of overestimation of pressure drop and effect on gFFR is unpredictable [28]. Hence, in clinical practice, it is suggested to use the FFR-gFFR or CFR-gCFR correlation to determine the true FFR or CFR from existing clinical measurements of gFFR and gCFR values measured by guidewire and conse-quently evaluate physiological ischemic conditions, particularly for intermediate stenosis regime signifying vulnerable lesion.

Guidewire flow-obstruction effect, which overestimates the functional degree of stenosis (by underestimating the true FFR and CFR), leads to erroneous conclusions and needless interventions. The guidewire insertion induced % error in gFFR measurement was approximately represented as $\{1-[R_v^2 P_s^2(R_v^2 P_s^2 -d_g^2/2)^{-1}]^2\}\times100$, where d_g is the guidewire diameter, P_s is the % diameter stenosis/100, and R_v is the vessel radius [5,29]. The 10–40% error was estimated in gFFR measurement for intermediate stenosis. Based on an in vitro study [8], it has been documented that (1) the influence of guidewire on stenosis hemodynamics is negligible in the range of stenoses where functional assessment is desirable and (2) the error in gFFR due to the guidewire insertion is appreciable only when gFFR is less than 0.75. However, based on our earlier numerical estimations [20–22,25], introduction of the guidewire produces a larger % difference in guidewire based measurement of $\Delta\tilde{p}$ above the pathophysiological values.

There are many variables which govern the gCFR or flow mea-

Table 4 Effect of guidewire and guiding catheter diameters on determining ischemic limits of gFFR and gCFR [30,33]. ET, exercise thallium test; DE, dipyridamole echo; A/DS, Adeno/dipysestamibi; DuE, dobutamine echo; ExT, exercise test; E ECG, exercise ECG.

Author	Noninvasive functional test	Limiting gCFR	Guidewire diameter (in.)	Guiding catheter diameter (F)	Comment
Heller et al. [35]	ET	<1.7	0.014	Not reported	55 patients with single stenosis in the proximal or mid portion
Miller et al. [36]	A/DS	<2	0.018	6	33 patients, single lesion, single vessel
		Limiting gFFR			
Pijls et al. [1]	4-test standard	<0.75	0.018	6–8	45 patients with moderate coronary stenosis and chest pain of uncertain origin
De Bruyne et al. [37]	E ECG	<0.72	0.015 or 0.018	7	60 patients with an isolated lesion in one major epicardial coronary artery
Bartunek et al. [38]	DuE	<0.68	0.014	Not reported	37 patients with single-vessel isolated epicardial lesion
Pijls et al. [4]	ExT	<0.74	0.018 or 0.014	6–8	60 patients with single-vessel disease

surement. Major parameters can be summarized as viscosity of blood with varying hematocrit [19], diffused stenosis length, multiple stenoses, microvascular dysfunction, and initial base line flow condition [30]. The effect of steady and pulsatile flow regime on trans-stenotic pressure drop has already been introduced in this experimental study, though effect of different flow wave form shapes needs to be studied in the future along with other parameters. All physiological changes from patient to patient are reflected on $CFR - \tilde{p}_{rh}$ line. This study is based on the $CFR - \tilde{p}_{rh}$ correlation reported previously [6,25], giving zero flow pressure $\tilde{p}_{zf} \approx 20$ mm Hg. However, distal microvascular resistance and collateral flow may change the hemodynamics of epicardial stenosis and $\tilde{p}_{zf}$. This change is observed with shift in $CFR - \tilde{p}_{rh}$ line, changing $\tilde{p}_{zf}$ from 15 mm Hg to 40 mm Hg [28]. Thus, to apply the FFR-gFFR and CFR-gCFR correlations for large patient groups, the effect of different $CFR - \tilde{p}_{rh}$ lines on these correlations should be studied further.

The indirect effect of guide catheter diameter in association with guidewire diameter on gFFR should be considered [28,31]. Although no significant difference was reported in clinical trials for 4F and 7F guiding catheters [32], the catheter diameter affects gFFR measurement in addition to the guidewire size [31]. This can be easily checked from the clinical data available for determining the limiting ischemic conditions of gFFR and gCFR with the use of guidewire (Table 4). It is assumed that the difference between the limiting ischemic gFFR and gCFR values, viz., 0.68–0.75 and 1.7–2, respectively, is due to various guidewire and catheter sizes used in these clinical trials. However, patient population, distal microvascular resistance, and different noninvasive stress test conditions may influence the limiting conditions of gFFR and gCFR.

The guidewire flow-obstruction effect is more significant in the diagnosis of mild to intermediate stenosis [28] whose occurrence is quite large in patients undergoing angioplasty [33]. Under such clinical settings, the decision making of performing angioplasty and stent placement or to defer these procedures becomes complex and difficult. To assess intermediate stenosis in the event of microvascular dysfunction, simultaneous gCFR and gFFR measurements are suggested. For this purpose, a pressure and Doppler flow guidewire were inserted simultaneously [34]. With single pressure guidewire, the gFFR was measured as 0.77. After insertion of Doppler guidewire, simultaneously measured gFFR and gCFR were 0.72 and 1.6, respectively. Extrapolating these clinical data, true FFR and CFR (without any guidewire insertion) would be greater than 0.77 and 1.6, respectively. However, with double guidewire insertion, FFR and CFR were reduced below the corresponding threshold values of 0.75 for FFR and 2 for CFR, respectively. To avoid this diagnostic conundrum, a new diagnostic parameter, LFC, is studied, which considers the effect of guidewire or catheter diameter in addition to simultaneously measured coronary trans-stenotic pressure drop and flow. However, more experiments are needed for intermediate area stenosis regime to get more accurate relations between physiological parameters such as gFFR, gCFR, and gLFC. Thus, in the future, diagnosis of intermediate stenosis may be carried out by using a single parameter, gLFC (Fig. 7).

Conclusion

There is larger difference between guidewire based and physiological or true measurement of pressure drops for stenosis test sections under steady and pulsatile flow conditions. Hence, pulsatile flow experiments are more physiologically appropriate than steady flow experiments. The guidewire insertion under steady or pulsatile flow alters the trans-stenotic hemodynamics differently. However, the FFR-gFFR and CFR-gCFR relations remain similar for steady and pulsatile flow conditions. These correlations match well with in vivo data and hence may be used in clinical practice to determine true FFR and CFR based on the measurement of guidewire based gFFR and gCFR. This will help to reduce the confusion during the diagnosis of severity of coronary stenosis. The newly developed diagnostic parameter (LFC) is also well correlated with FFR and CFR for preangioplasty and postangioplasty stenoses in these in vitro experiments, justifying its possible clinical use.

Nomenclature

$$\% \text{ area stenosis} = 1 - [(A_m - A_g)/(A_e - A_g)] \times 100$$
$$= 1 - [(d_m^2 - d_g^2)/(d_e^2 - d_g^2)] \times 100;$$

without guidewire, $A_g = d_g = 0$

$A = \pi d^2/4$ = flow cross-sectional area

CFR = ratio of mean coronary flow at hyperemia to mean coronary flow at rest $= \tilde{Q}_h/\tilde{Q}_b$

d = diameter of vessel

FFR = myocardial fractional flow reserve $= (\tilde{p}_{\text{rh}} - \tilde{p}_v)/(\tilde{p}_a - \tilde{p}_v);$

$\tilde{p}_v$ = central venous pressure ~ 0 mm Hg

l = length of vessel

p = coronary pressure

Q = coronary flow

r = radius of vessel

Re_e = proximal Reynolds number $= \rho v_e d_e/\mu_\infty$

Re_m = throat Reynolds number $= \rho v_m d_m/\mu_\infty$

v = blood velocity

$\Delta p = p_a - p_r$ = trans-stenotic pressure drop

V = velocity component

$\kappa = A_m/A_e$ or $(A_m - A_g)/(A_e - A_g)$ = area ratio

ρ = density of blood

σ_u = ultimate tensile strength (ASTM D 638)

μ = dynamic viscosity

ν = kinematic viscosity

Subscript

a = proximal aortic pressure

b = base line flow condition

c = constriction section

e = proximal nonstenosed vessel lumen

h = pharmacologically induced hyperemia

g = guidewire

m = minimum stenosis lumen

r = distal region to the stenosis

rh = recovered hyperemic pressure distal to the stenosis

zf = zero flow

Superscript

$\sim$ = time averaged physiological quantity (pressure or flow)

g = guidewire; FFR or CFR measured by inserting sensor tipped guidewire through stenosed vessel

Appendix

Sources of errors between numerical and experimental results are follows.

(1) During in vitro experiments, guidewire may be eccentric with respect to the stenosis walls, showing asymmetric configuration. Also, guidewire oscillates inside the stenosis test section due to pulsatile flow. The concentric configuration of guidewire placement, which is assumed in numerical calculations, results in higher $\Delta \tilde{p}$ (worst case scenario) than eccentric placement of guidewire across the stenosis, as in the case of experimental measurements, for the same mean flow rate.

(2) All dimensions are measured with MicroCT, having an accuracy of 37 μm. In preangioplasty stenosis regions, small change in d_m and l_m will change the pressure drop appreciably [8].

(3) Assumption of axisymmetric model. The experimental geometry is assumed as axisymmetric for computational validation. However, the geometries of manufactured test sections are not exactly axisymmetric as per MicroCT images (Fig. 1).

(4) Viscosity of BAF. The viscosity of BAF ($\mu_0 = 55.72$ cP, $\mu_\infty = 3.39$ cP, $\lambda = 9.67$ s, $n = 0.2$) is somewhat lower than the blood ($\mu_0 = 56$ cP, $\mu_\infty = 3.45$ cP, $\lambda = 3.313$ s, $n = 0.3568$) [19]. Due to the lower viscosity of BAF, rigorous numerical technique is needed for computational stability. The higher viscosity will further stabilize the numerical computations as well as experimental data.

(5) Pressure scanner accuracy, ± 0.5 mm Hg.

(6) The shear layer instabilities detected in 80% and 90% area stenosis [20].

(7) Dimensions (length and diameter) of pressure port and their axial positions. Due to flow separation and vortex formation in the distal region, streamlines are not parallel to the vessel wall and are not perpendicular to the pressure port axis in the distal region.

References

[1] Pijls, N. H., De Bruyne, B., Peels, K., Van der Voort, P. H., Bonnier, H. J., Bartunek, J., and Koolen, J. J., 1996, "Measurement of Fractional Flow Reserve to Assess the Functional Severity of Coronary-Artery Stenoses," N. Engl. J. Med., **334**(26), pp. 1703–1708.

[2] Gould, K. L., Lipscomb, K., and Hamilton, G. W., 1974, "Physiologic Basis for Assessing Critical Coronary Stenosis. Instantaneous Flow Response and Regional Distribution During Coronary Hyperemia as Measures of Coronary Flow Reserve," Am. J. Cardiol., **33**(1), pp. 87–94.

[3] Siebes, M., Verhoeff, B. J., Meuwissen, M., de Winter, R. J., Spaan, J. A., and Piek, J. J., 2004, "Single-Wire Pressure and Flow Velocity Measurement to Quantify Coronary Stenosis Hemodynamics and Effects of Percutaneous Interventions," Circulation, **109**(6), pp. 756–762.

[4] Pijls, N. H., Van Gelder, B., Van der Voort, P., Peels, K., Bracke, F., Bonnier, H. J., and el Gamal, M. I., 1995, "Fractional Flow Reserve. A Useful Index to Evaluate the Influence of an Epicardial Coronary Stenosis on Myocardial Blood Flow," Circulation, **92**(11), pp. 3183–3193.

[5] Pijls, N. H., and De Bruyne, B., 1998, "Coronary Pressure Measurement and Fractional Flow Reserve," Heart, **80**(6), pp. 539–542.

[6] Wilson, R. F., Johnson, M. R., Marcus, M. L., Alyward, P. E., Skorton, D. J., Collins, S., and White, C. W., 1988, "The Effect of Coronary Angioplasty on Coronary Flow Reserve," Circulation, **77**(4), pp. 873–885.

[7] Anderson, H. V., Roubin, G. S., Leimgruber, P. P, Cox, W. R., Douglas, J. S., King, S. B., and Gruentzig, A. R., 1986, "Measurement of Transstenotic Pressure Gradient During Percutaneous Transluminal Coronary Angioplasty," Circulation, **73**(6), pp. 1223–1230.

[8] De Bruyne, B., Pijls, N. H., Paulus, W. J., Vantrimpont, P. J., Sys, S. U., and Heyndrickx, G. R., 1993, "Transstenotic Coronary Pressure Gradient Measurement in Humans: *In Vitro* and *In Vivo* Evaluation of a New Pressure Monitoring Angioplasty Guide Wire," J. Am. Coll. Cardiol., **22**(1), pp. 119–126.

[9] Ganz, P., Harrington, D. P., Gaspar, J., and Barry, W. H., 1983, "Phasic Pressure Gradients Across Coronary and Renal Artery Stenoses in Humans," Am. Heart J., **106**(6), pp. 1399–1406.

[10] Doucette, J. W., Corl, P. D., Payne, H., Flynn, A. E., Goto, M., Nassi, M., and Segal, J., 1992, "Validation of a Doppler Guide Wire for Intravascular Measurement of Coronary Artery Flow Velocity," Circulation, **85**(5), pp. 1899–1911.

[11] Back, L. H., Kwack, E. Y., and Back, M. R., 1996, "Flow Rate-Pressure Drop Relation in Coronary Angioplasty: Catheter Obstruction Effect," ASME J. Biomech. Eng., **118**(1), pp. 83–89.

[12] Emanuelsson, H., Dohnal, M., Lamm, C., and Tenerz, L., 1991, "Initial Experiences with a Miniaturized Pressure Transducer During Coronary Angioplasty," Cathet Cardiovasc. Diagn., **24**(2), pp. 137–143.

[13] Back, L. H., 1994, "Estimated Mean Flow Resistance Increase During Coronary Artery Catheterization," J. Biomech., **27**(2), pp. 169–175.

[14] Jenni, R., Buchi, M., Zweifel, H. J., and Ritter, M., 1998, "Impact of Doppler Guidewire Size and Flow Rates on Intravascular Velocity Profiles," Cathet Cardiovasc. Diagn., **45**(1), pp. 96–100.

[15] Pijls, N. H. J., 2003, "Is It Time to Measure Fractional Flow Reserve in All Patients?," J. Am. Coll. Cardiol., **41**(7), pp. 1122–1124.

[16] Banerjee, R. K., Sinha Roy, A., Back, L. H., Back, M. R., Khoury, S. F., and Millard, R. W., 2007, "Characterizing Momentum Change and Viscous Loss of a Hemodynamic Endpoint in Assessment of Coronary Lesions," J. Biomech., **40**(3), pp. 652–663.

[17] Cho, Y. I., Back, L. H., Crawford, D. W., and Cuffel, R. F., 1983, "Experimental Study of Pulsatile and Steady Flow Through a Smooth Tube and an Atherosclerotic Coronary Artery Casting of Man," J. Biomech., **16**(11), pp. 933–946.

[18] Brookshier, K. A., and Tarbell, J. M., 1993, "Evaluation of a Transparent Blood Analog Fluid: Aqueous Xanthan Gum/Glycerin," Biorheology, **30**(2), pp. 107–116.

[19] Cho, Y. I., and Kensey, K. R., 1991, "Effects of the Non-Newtonian Viscosity of Blood on Flows in a Diseased Arterial Vessel. Part 1: Steady Flows," Biorheology, **28**(3–4), pp. 241–262.

[20] Banerjee, R. K., Back, L. H., and Back, M. R., 2003, "Effects of Diagnostic Guidewire Catheter Presence on Translesional Hemodynamic Measurements Across Significant Coronary Artery Stenoses," Biorheology, **40**(6), pp. 613–635.

[21] Banerjee, R. K., Back, L. H., Back, M. R., and Cho, Y. I., 2003, "Physiological Flow Analysis in Significant Human Coronary Artery Stenoses," Biorheology, **40**(4), pp. 451–476.

[22] Banerjee, R. K., Back, L. H., Back, M. R., and Cho, Y. I., 2000, "Physiological Flow Simulation in Residual Human Stenoses After Coronary Angioplasty," ASME J. Biomech. Eng., **122**(4), pp. 310–320.

[23] Young, D. F., and Tsai, F. Y., 1973, "Flow Characteristics in Models of Arterial Stenoses-I Steady Flow; II Unsteady Flow," J. Biomech., **6**(4), pp. 395–410; , **6**(5), pp. 547–559.

[24] Gould, K. L., 1988, "Identifying and Measuring Severity of Coronary Artery Stenosis. Quantitative Coronary Arteriography and Positron Emission Tomography," Circulation, **78**(2), pp. 237–245.

[25] Sinha Roy, A., Banerjee, R. K., Back, L. H., Back, M. R., Khoury, S., and Millard, R. W., 2005, "Delineating the Guide-Wire Flow Obstruction Effect in Assessment of Fractional Flow Reserve and Coronary Flow Reserve Measurements," Am. J. Physiol. Heart Circ. Physiol., **289**(1), pp. H392–H397.

[26] Brown, B. G., Bolson, E. L., and Dodge, H. T., 1984, "Dynamic Mechanisms in Human Coronary Stenosis," Circulation, **70**(6), pp. 917–922.

[27] Takayama, T., and Hodgson, J. M., 2001, "Prediction of the Physiologic Severity of Coronary Lesions Using 3D IVUS: Validation by Direct Coronary Pressure Measurements," Catheter Cardiovasc. Interv., **53**(1), pp. 48–55.

[28] Pijls, N. H. J., and De Bruyne, B., 2000, *Coronary Pressure*, 2nd ed., Kluwer Academic, Dordrecht.

[29] Poullis, M., 1999, "Coronary Pressure Measurements: Catheter Induced Errors," Letters to the Editor, Heart, **82**(5), pp. 644–645.

[30] Kern, M. J., 2000, "Coronary Physiology Revisited: Practical Insights from the Cardiac Catheterization Laboratory," Circulation, **101**(11), pp. 1344–1351.

[31] Pijls, N. H., Kern, M. J., Yock, P. G., and De Bruyne, B., 2000, "Practice and Potential Pitfalls of Coronary Pressure Measurement," Catheter Cardiovasc. Interv., **49**(1), pp. 1–16.

[32] Legalery, P., Seronde, M., Meneveau, N., Schiele, F., and Bassand, J. P., 2003, "Measuring Pressure-Derived Fractional Flow Reserve Through Four French Diagnostic Catheters," Am. J. Cardiol., **91**(9), pp. 1075–1078.

[33] Patil, C. V., and Beyar, R., 2000, "Intermediate Coronary Artery Stenosis: Evidence-Based Decisions in Interventions to Avoid the Oculostenotic Reflex," Int. J. Cardiovasc Intervent, **3**(4), pp. 195–206.

[34] Ruiz-Salmeron, R. J., Goicolea, J., Sanmartin, M., Mantilla, R., Sterling, J., and Romeo, D., 2002, "Simultaneous Intracoronary Pressure and Doppler Guidewires to Assess Coronary Stenosis: If One is Enough, Are Two Too Much?," Catheter Cardiovasc. Interv., **55**(2), pp. 255–259.

[35] Heller, L. I., Cates, C., Popma, J., Deckelbaum, L. I., Joye, J. D., Dahlberg, S. T., Villegas, B. J., Arnold, A., Kipperman, R., Grinstead, W. C., Balcom, S., Ma, Y., Cleman, M., Steingart, R. M., and Leppo, J. A., 1997, "Intracoronary Doppler Assessment of Moderate Coronary Artery Disease: Comparison with 201Tl Imaging and Coronary Angiography. FACTS Study Group," Circulation, **96**(2), pp. 484–490.

[36] Miller, D. D., Donohue, T. J., Younis, L. T., Bach, R. G., Aguirre, F. V., Wittry, M. D., Goodgold, H. M., Chaitman, B. R., and Kern, M. J., 1994, "Correlation of Pharmacological 99mTc-Sestamibi Myocardial Perfusion Imaging with Poststenotic Coronary Flow Reserve in Patients With Angiographically Intermediate Coronary Artery Stenoses," Circulation, **89**(5), pp. 2150–2160.

[37] De Bruyne, B., Bartunek, J., Sys, S. U., and Heyndrickx, G. R., 1995, "Relation Between Myocardial Fractional Flow Reserve Calculated from Coronary Pressure Measurements and Exercise-Induced Myocardial Ischemia," Circulation, **92**(1), pp. 39–46.

[38] Bartunek, J., Van Schuerbeeck, E., and De Bruyne, B., 1997, "Comparison of Exercise Electrocardiography and Dobutamine Echocardiography with Invasively Assessed Myocardial Fractional Flow Reserve in Evaluation of Severity of Coronary Arterial Narrowing," Am. J. Cardiol., **79**(4), pp. 478–481.